Determining the chirality of Weyl fermions from circular dichroism spectra in time-dependent angle-resolved photoemission

Rui Yu,[1,*] Hongming Weng,[2,3] Zhong Fang,[2,3] Hong Ding,[2,3] and Xi Dai[2,3,†]

[1]*Department of Physics, Harbin Institute of Technology, Harbin 150001, China*

[2]*Beijing National Laboratory for Condensed Matter Physics, Institute of Physics, Chinese Academy of Sciences, Beijing 100190, China*

[3]*Collaborative Innovation Center of Quantum Matter, Beijing 100190, China*

(Received 14 December 2015; published 18 May 2016)

We show that the intensity of pumped states near Weyl point is different when pumped with left- and right-handed circular-polarized light, which leads to a special circular dichroism (CD) in time-dependent angle-resolved photoemission spectra (ARPES). We derive the expression for the CD of time-dependent ARPES, which is directly related to the chirality of Weyl fermions. Based on the above derivation, we further propose a method to determine the chirality for a given Weyl point from the CD of time-dependent ARPES. The corresponding CD spectra for TaAs has then been calculated from first principles, which can be compared with future experiments.

DOI: 10.1103/PhysRevB.93.205133

I. INTRODUCTION

The research on topological quantum states has emerged as one of the major topics in condensed matter physics in recent years. It was ignited by the discovery of two-dimensional (2D) and three-dimensional (3D) topological insulators (TIs) [1,2] and received significant attention again by the discovery of 3D topological semimetals. In 3D topological semimetals, the conduction and valence bands touch at certain points in the Brillouin zone and generate nontrivial band topology [3]. Up to now, there are three types of topological semimetals: Weyl semimetals, Dirac semimetals, and node-line semimetals. For Weyl semimetals, the band touching points are doubly degenerate and distributed in the Brillouin zone as isolated points, which can be viewed as "magnetic monopoles" in momentum space [4]. According to the so-called "no-go theorem" [5–7], Weyl points in lattice systems always appear in pairs with definite and opposite chirality. The Dirac semimetals can be generated by overlapping two Weyl fermions with opposite chirality at the same k-point, which has fourfold degenerate at the band touching points and can be only protected by additional crystalline symmetry [8,9]. For node-line semimetals, the band touching points form closed loops in Brillouin zone around the Fermi level [10–13].

The breakthrough in topological semimetals research happened after the material realization of Dirac semimetal states in Na_3Bi and Cd_3As_2 [8,9,14–18]. Starting from Dirac semimetals, one can obtain Weyl semimetals by breaking either time-reversal [19–22] or inversion symmetry [23–27]. Recently, a family of nonmagnetic and noncentrosymmetric 3D Weyl semimetals, the stoichiometric TaAs, TaP, NbAs, and NbP, was first predicted theoretically [28,29] and then verified experimentally [30–37]. The intriguing expected properties characterizing a Weyl semimetal have been checked carefully in this family of materials. The surface Fermi arcs have been observed in most of these materials from ARPES experiments [30,31,34–37]. The nontrivial π Berry's phase has been experimentally accessed by analyzing the Shubnikov de Haas oscillations in TaAs [33,38]. The negative magnetoresistivity due to the chiral anomaly has been observed in TaAs [33]. However, all the above experiments can only prove the existence of the Weyl points but can not determine the chirality for each particular Weyl point, which is a key issue in the physics of Weyl semimetals. In this paper, we show that the chirality of a particular Weyl point can be determined from the CD spectra of the time-dependent ARPES experiment, which is a powerful tool for investigating the spin, orbital, and valley property of electrons in crystalline materials [39–42].

II. WEYL HAMILTONIAN

The most general Hamiltonian expanded near a Weyl point can be expressed by the following two-band model:

$$H_W = \sum_{i,j} k_i a_{ij} \sigma_j = (k_x,k_y,k_z)\hat{a}(\sigma_x,\sigma_y,\sigma_z)^T, \qquad (1)$$

where $i,j = x,y,z$ and the matrix a connects the pseudospin space σ and momentum space $\mathbf{k}$. Equation (1) can be rewritten as

$$H_W = \chi \sum_{i,j} k_i \tilde{a}_{ij} \sigma_j, \qquad (2)$$

where $\chi = \mathrm{sign}[\mathrm{Det}(a)]$ is the chirality of the Weyl fermions. The new matrix $\tilde{a}$ is defined as $\tilde{a} = \chi a$ and has a positive determinant $\mathrm{sign}[Det(\tilde{a})] = +1$. The matrix $\tilde{a}$ can be decomposed by single-value decomposition (SVD) as $\tilde{a} = S\Lambda D$, where Λ is a diagonal matrix with three positive elements denoted as λ_1, λ_2, and λ_3. S and D are two real orthogonal matrices and we can choose a gauge condition that both of them have positive determinants, with which the new coordinates can be uniquely defined according to the "principal axes" in the momentum and pseudospin spaces as $(k_1,k_2,k_3) = (k_x,k_y,k_z)S$ and $(\sigma_1,\sigma_2,\sigma_3) = (\sigma_x,\sigma_y,\sigma_z)D^T$, respectively.

Rotating the coordinate systems into the principal axis defined as 1, 2, and 3 in both momentum and pseudospin spaces, Eq. (2) can be rewritten as

$$H_W = \chi \sum_{i=1,2,3} \lambda_i k_i \sigma_i. \qquad (3)$$

*yurui@hit.edu.cn
†daix@iphy.ac.cn

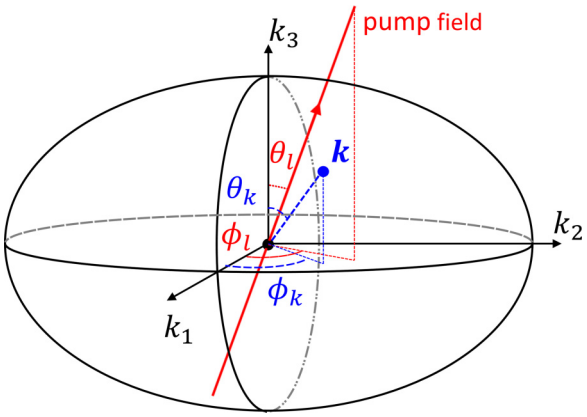

FIG. 1. Diagram of the experimental geometry. Circular-polarized light can be continuously rotated by θ_l and ϕ_l as shown in the figure.

In Weyl semimetal materials, the Weyl points always come in pairs with opposite chirality. In the following sections, we will discuss how to detect the chirality for a given Weyl point from the CD of a time-dependent ARPES experiment. In the experimental setup, as illustrated in Fig. 1, we shine circular-polarized light onto a Weyl semimetal in order to pump electrons from the occupied states to the unoccupied states. Since the purpose is to selectively pump the "chiral electrons" from the lower branch to the upper branch of a Weyl cone using chiral photons (see Fig. 2) [42,43], the energy of the pumping photons needs to be within the linear range of the Weyl dispersion, which is roughly a few tens meV for TaAs, thus a THz source is required. The continuously pumped unoccupied states can then be probed by regular bulk-sensitive ARPES, such as soft x-ray ARPES, commonly used in the study of Weyl semimetals [30,31,34–37].

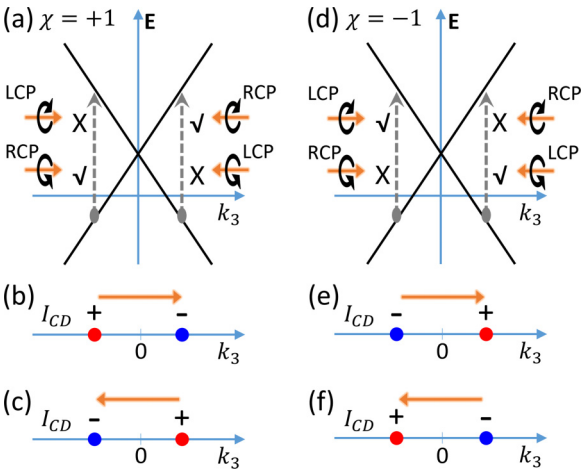

FIG. 2. (a) In the condition of $\lambda_1 = \lambda_2$, for the Weyl fermions with chirality $\chi = 1$, the occupied states in the $+\hat{k}_3$ axis can only be pumped to the empty states by left (right)-handed circular-polarized light incident along the $\hat{k}_3$ ($-\hat{k}_3$) direction, while for the states in the $-\hat{k}_3$ axis, they can only be pumped by right (left)-circular-polarized light incident along the $\hat{k}_3$ ($-\hat{k}_3$) direction. (b) and (c) The CD values with light incident along the $\hat{k}_3$ and $-\hat{k}_3$ direction for $\chi = 1$. The CD value is only determined by the relative direction between the electronic momentum $\mathbf{k}$ and the propagating direction of the light. It is positive (negative) for $\mathbf{k}$ antiparallel (parallel) to the propagating direction of the light. (d)–(f) for the Weyl fermions with chirality $\chi = -1$. The CD value is positive (negative) for $\mathbf{k}$ parallel (antiparallel) to the propagating direction of the light.

III. CD SPECTRA OF PUMPED STATES

We start from the Hamiltonian (3) and take $\chi = +1$ as an example to discuss the CD spectra of pumped states for Weyl fermions. The eigenvalues of Eq. (3) are given as $E_{c/v} = \pm((\lambda_1 k_1)^2 + (\lambda_2 k_2)^2 + (\lambda_3 k_3)^2)^{1/2}$, and the eigenfunctions for conduction and valence bands are given as

$$|u_c\rangle = \begin{bmatrix} \cos\frac{\theta_k}{2} e^{-i\frac{\phi_k}{2}} \\ \sin\frac{\theta_k}{2} e^{+i\frac{\phi_k}{2}} \end{bmatrix} \text{ and } |u_v\rangle = \begin{bmatrix} -\sin\frac{\theta_k}{2} e^{-i\frac{\phi_k}{2}} \\ +\cos\frac{\theta_k}{2} e^{+i\frac{\phi_k}{2}} \end{bmatrix}, \quad (4)$$

where $\cos\theta_k = \frac{\lambda_3 k_3}{|E|}$ and $\tan\phi_k = \frac{\lambda_2 k_2}{\lambda_1 k_1}$.

To consider the coupling of electrons and pump light, we start from the microscopic Hamiltonian of an electron with spin-orbit coupling, which is given by

$$H_0 = \frac{\mathbf{p}^2}{2m} + V + \frac{\hbar}{4m^2}(\nabla V \times \mathbf{p}) \cdot \mathbf{s}, \quad (5)$$

where $\mathbf{p}$ is the momentum operator, V is the crystal potential, and $\mathbf{s}$ is the electron spin operator. The Hamiltonian for systems coupled to the electromagnetic field is obtained via the Peierls substitution $\mathbf{p} \to \mathbf{p} - e\mathbf{A}$, where $\mathbf{A}$ is the vector potential of the electromagnetic field. The electron-photon interaction term can then be obtained as $H_{\text{int}} = H_0(\mathbf{p} - e\mathbf{A}) - H_0(\mathbf{p})$ leading to

$$H_{\text{int}} = -e\mathbf{A} \cdot \mathbf{v}, \quad (6)$$

where

$$v_i = \frac{\partial H_W}{\partial k_i} = \chi \lambda_i \sigma_i, \quad (7)$$

is the velocity operator, where $i = 1,2,3$.

Suppose in the ideal case the chemical potential is located right at the Weyl point, then the pumping rate from the lower branch to the upper branch caused by the light is determined by the following matrix element:

$$M_{cv} = \langle u_c | \mathcal{A} \cdot \mathbf{v} | u_v \rangle, \quad (8)$$

where $\mathcal{A}$ is the Fourier transform of vector potential $\mathbf{A}$. For the circular-polarized light, we have

$$\begin{aligned} \mathcal{A}_x &= A_0(\cos\theta_l \cos\phi_l + \eta i \sin\phi_l), \\ \mathcal{A}_y &= A_0(\cos\theta_l \sin\phi_l - \eta i \cos\phi_l), \\ \mathcal{A}_z &= -A_0 \sin\theta_l, \end{aligned} \quad (9)$$

where $\eta = \pm 1$ indicate the right/left-handed circular-polarized light and θ_l and ϕ_l are angles describing the propagating direction of the injecting light as illustrated in Fig. 1.

First, we consider the simplest case with the light incident along one of the principal axis, say along $\hat{k}_3$ axis with $\theta_l = 0$ and $\phi_l = 0$. The vector potential of light in Eq. (9) is then simplified as

$$\mathcal{A} = A_0(1, -\eta i, 0). \quad (10)$$

Therefore the matrix element in Eq. (8) can be written as

$$M_{cv} = \langle u_c|\tfrac{1}{2}(\mathcal{A}_- v_+ + \mathcal{A}_+ v_-)|u_v\rangle, \tag{11}$$

where $\mathcal{A}_\pm = \mathcal{A}_1 \pm i\mathcal{A}_2 = A_0(1 \pm \eta)$ and $v_\pm = v_1 \pm i v_2$. For the states in the $+\hat{k}_3$ axis, where $\theta_k = 0$, we get $|u_c\rangle_{+\hat{k}_3} = \binom{1}{0}$ and $|u_v\rangle_{+\hat{k}_3} = \binom{0}{1}$ as expressed in Eq. (4). To keep the discussions simple, we suppose that $\lambda_1 = \lambda_2$. Then it is easy to check that only the v_+ operator contributes a nonzero matrix element between $|u_c\rangle_{+\hat{k}_3}$ and $|u_v\rangle_{+\hat{k}_3}$ states. Meanwhile, the requirement of $\mathcal{A}_-$ being nonzero leads to $\eta = -1$. These results mean that for Weyl fermions with chirality $\chi = 1$, the occupied states in the $+\hat{k}_3$ axis can only be pumped by the left-handed circular-polarized photons. For the states in the $-\hat{k}_3$ axis, they can only be pumped by the right-handed circular-polarized photons as illustrated in Fig. 2(a). Whereas for $\chi = -1$, with the same argument as discussed above, we find that the situation is just the opposite, where the states at the $\pm\hat{k}_3$ axis can only be pumped by the right/left-handed circular-polarized light as illustrated in Fig. 2(d).

The pumping process induced by the circular-polarized light will be eventually balanced by the relaxation processes in the crystal and form a steady state. The occupation intensity of the exited states in such a steady state can be obtained as [44]

$$I_\eta \propto |M_{cv}|^2 A_c(E_c) A_v(E_v) = |M_{cv}|^2/(\pi^2 \epsilon_c \epsilon_v), \tag{12}$$

where $A_v(\omega) = \frac{1}{\pi}\frac{\epsilon_v}{[\omega - E_v]^2 + \epsilon_v^2}$ and $A_c(\omega) = \frac{1}{\pi}\frac{\epsilon_c}{[\omega - E_c]^2 + \epsilon_c^2}$ denote the spectral functions of the initial and final states in the noninteracting case. The parameters ϵ_v and ϵ_c reflect the finite lifetime of electrons. The CD spectra are defined as $I_{\rm CD} = I_{\rm RCP} - I_{\rm LCP}$, which measures the difference of I with right- and left-handed circular-polarized pumping light. Therefore the CD values in the $\pm\hat{k}_3$ axis can be calculated as

$$I_{\rm CD}^{\pm\hat{k}_3} \propto \mp 4\chi A_0^2 \lambda_1^2/(\pi^2 \epsilon_c \epsilon_v), \tag{13}$$

which shows that the CD spectra take opposite values at $\pm\hat{k}_3$ axis and its sign is directly related to the chirality χ as shown in Figs. 2(b) and 2(e).

The above results indicate that we can determine the chirality for a given Weyl point by checking the CD of time-dependent ARPES. However, there is one problem that needs to be clarified. In the previous paragraph, we have set the light propagating direction to be identical to the positive direction of the absolute coordinate system and obtain the above results. It seems that we need to know in advance which direction is positive (according to the gauge fixing condition defined above) for a given principal axis, which is not possible experimentally. Actually, this is not necessary due to the following reason. Let us consider another possibility that the circular polarized light is applied antiparallel to the absolute $\hat{k}_3$ direction. The CD spectra can be obtained as shown in Figs. 2(c) and 2(f). Comparing the results in Figs. 2(b), 2(c), 2(e), and 2(f), we find that if we define the propagating direction of the circular-polarized light as the reference direction, the results for both situations become identical, namely for a Weyl point with chirality $\chi = 1$ the CD of the time-dependent ARPES will be positive (negative) for momentum $\mathbf{k}$ antiparallel (parallel) to the propagating direction of light as illustrated in Figs. 2(b) and 2(c), while for $\chi = -1$ the CD spectra will be positive (negative) for momentum $\mathbf{k}$ parallel (antiparallel) to the propagating direction of light as illustrated in Figs. 2(e) and 2(f). Therefore the above results can be used to determine the chirality of a Weyl point purely by experiments.

For the more general case with the pump field injected at angles θ_l and ϕ_l, the CD spectra at $\mathbf{k}$ point with angles θ_k and ϕ_k can be calculated as

$$I_{\rm CD} \propto -4\chi A_0^2(\lambda_1\lambda_2 \cos\theta_k \cos\theta_l + \lambda_3 \sin\theta_k \sin\theta_l \times(\lambda_2 \cos\phi_k \cos\phi_l + \lambda_1 \sin\phi_k \sin\phi_l))/(\pi^2 \epsilon_c \epsilon_v). \tag{14}$$

We discuss the CD spectra for the general case in the following section.

IV. WEYL POINTS IN TAAS

The new discovered TaAs family materials are the first verified realistic materials that contain Weyl points near the Fermi level. Totally, there are 12 pairs of Weyl points in TaAs as shown in Fig. 3(a). The two nonequivalent pairs are marked as W1 and W2. At each Weyl point, the low-energy effective Hamiltonian takes the form expressed in Eq. (1). The matrix a in Eq. (1) for W1 and W2 can be obtained by fitting with the first-principles calculations and can be expressed as

$$a^{W1} = \begin{bmatrix} 2.657 & -2.526 & 0.926 \\ 0.393 & -2.134 & 3.980 \\ -1.200 & -3.530 & 1.193 \end{bmatrix} \tag{15}$$

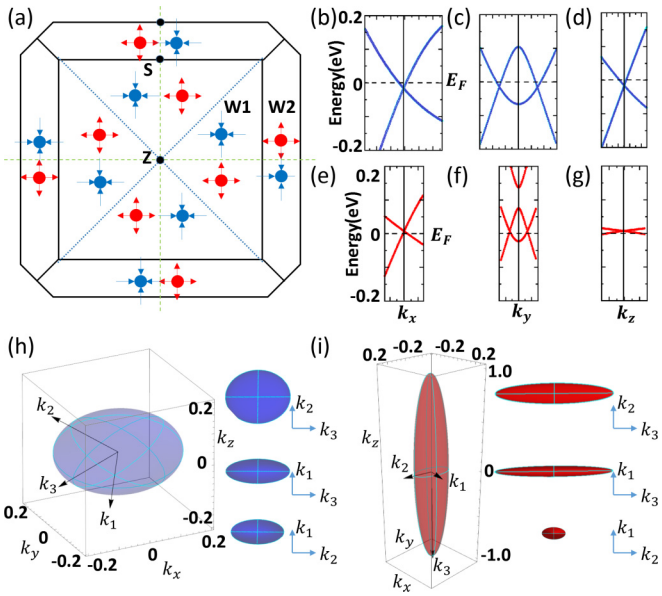

FIG. 3. (a) The distribution of the 12 pairs of Weyl points in BZ for TaAs compounds. We depict with red color the Weyl point with chirality $\chi = 1$ and bluecolor for $\chi = -1$. The two nonequivalent pairs are marked as W1 and W2. The four pairs of W1-type Weyl points shown in (a) are on the top of another four W1 pairs, which are invisible. The band dispersion near W1 and W2 points is shown in (b)–(d) and (e)–(g), respectively. (h) and (i) The ellipse-shaped isoenergetic surface near W1 and W2 points and their top view along three principal axes.

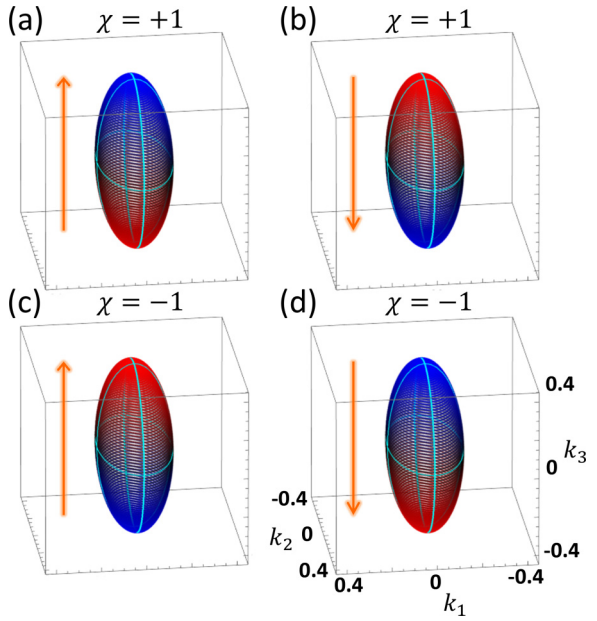

FIG. 4. The CD spectra for a Weyl point with chirality $\chi = 1$ pumped with field (a) parallel and (b) antiparallel to $+\hat{k}_3$ principal axis. The red color indicates the positive CD values and the blue color indicates negative CD values. In this case, the positive (negative) CD values are in the antiparallel (parallel) direction of the propagating direction of the light. (c) and (d) for a Weyl point with chirality $\chi = -1$. In this case, the positive (negative) CD values are in the parallel (antiparallel) direction of the propagating direction of the light.

and

$$a^{W2} = \begin{bmatrix} 1.849 & 2.531 & 0.269 \\ 1.849 & 1.388 & -4.910 \\ 0.428 & -0.302 & 0.006 \end{bmatrix}. \quad (16)$$

The energy dispersion and the isoenergetic surface near W1 and W2 are shown in Figs. 3(b)–3(i). By performing the SVD, we can get the singular values of a^{W1} and a^{W2} as $\lambda_1^{W1} = 6.055$, $\lambda_2^{W1} = 2.834$, $\lambda_3^{W1} = 2.340$, $\lambda_1^{W2} = 5.564$, $\lambda_2^{W2} = 2.899$, and $\lambda_3^{W2} = 0.520$ in units of eV Bohr. The principal axes of the ellipse for the isoenergetic surface near W1 and W2 are obtained as $\hat{k}_1^{W_1} = -(0.478,0.694,0.537)$, $\hat{k}_2^{W_1} = (-0.811,0.115,0.573)$, $\hat{k}_3^{W_1} = (-0.336,0.710,-0.618)$, $\hat{k}_1^{W_2} = (0.257,0.966,0.011)$, $\hat{k}_2^{W_2} = (0.966, -0.257, -0.007)$ and $\hat{k}_3^{W_2} = (-0.004,0.012, -0.999)$ as shown in Figs. 3(h) and 3(i).

With the help of Eq. (14), The CD spectra of time-dependent ARPES for a Weyl point can be obtained as

$$I_{\mathrm{CD}} \propto -4\chi A_0^2 \lambda_1 \lambda_2 \cos\theta_k / (\pi^2 \epsilon_c \epsilon_v), \quad (17)$$

with the pump field injected along the $\hat{k}_3$ direction. For the pump field injected along the $-\hat{k}_3$ direction, the CD spectra are

$$I_{\mathrm{CD}} \propto +4\chi A_0^2 \lambda_1 \lambda_2 \cos\theta_k / (\pi^2 \epsilon_c \epsilon_v). \quad (18)$$

Using the criterion discussed in the previous paragraph, the positive (negative) CD values for **k** antiparallel (parallel) to the propagating direction of the light indicate that $\chi = +1$, whereas the positive (negative) CD values for **k** parallel (antiparallel) to the propagating direction of the light indicate that $\chi = -1$ as shown in Fig. 4. This criterion works even when the light propagating direction slightly deviates from the principal axis.

V. CONCLUSION

In summary, we have investigated the CD of time-dependent ARPES near Weyl points and show that the CD values are related to the chirality of Weyl fermions, which provides a way to determine the chirality of a given Weyl point by checking the sign of the CD values along the propagating direction of the light. The corresponding CD spectra for a Weyl point in TaAs have then been calculated, which can be compared with future CD time-dependent ARPES experiments.

ACKNOWLEDGMENTS

This work was supported by the 973 program of China (Grant No. 2013CB921700) and the "Strategic Priority Research Program (B)" of the Chinese Academy of Sciences (No. XDB07020100). R.Y. acknowledges funding form the Fundamental Research Funds for the Central Universities (Grant No. AUGA5710059415) and the National Thousand Young-Talents Program.

[1] M. Z. Hasan and C. L. Kane, Rev. Mod. Phys. **82**, 3045 (2010).
[2] X.-L. Qi and S.-C. Zhang, Rev. Mod. Phys. **83**, 1057 (2011).
[3] G. E. Volovik, *The Universe in a Helium Droplet* (Clarendon Press, Oxford, 2003).
[4] Z. Fang, N. Nagaosa, K. S. Takahashi, A. Asamitsu, R. Mathieu, T. Ogasawara, H. Yamada, M. Kawasaki, Y. Tokura, and K. Terakura, Science **302**, 92 (2003).
[5] H. Nielsen and M. Ninomiya, Phys. Lett. B **105**, 219 (1981).
[6] H. Nielsen and M. Ninomiya, Nucl. Phys. B **185**, 20 (1981).
[7] H. Nielsen and M. Ninomiya, Nucl. Phys. B **193**, 173 (1981).
[8] Z. Wang, Y. Sun, X.-Q. Chen, C. Franchini, G. Xu, H. Weng, X. Dai, and Z. Fang, Phys. Rev. B **85**, 195320 (2012).
[9] Z. Wang, H. Weng, Q. Wu, X. Dai, and Z. Fang, Phys. Rev. B **88**, 125427 (2013).
[10] A. A. Burkov, M. D. Hook, and L. Balents, Phys. Rev. B **84**, 235126 (2011).
[11] H. Weng, Y. Liang, Q. Xu, R. Yu, Z. Fang, X. Dai, and Y. Kawazoe, Phys. Rev. B **92**, 045108 (2015).
[12] Y. Kim, B. J. Wieder, C. L. Kane, and A. M. Rappe, Phys. Rev. Lett. **115**, 036806 (2015).
[13] R. Yu, H. Weng, Z. Fang, X. Dai, and X. Hu, Phys. Rev. Lett. **115**, 036807 (2015).
[14] A. Pariari, P. Dutta, and P. Mandal, Phys. Rev. B **91**, 155139 (2015).

[15] L. P. He, X. C. Hong, J. K. Dong, J. Pan, Z. Zhang, J. Zhang, and S. Y. Li, Phys. Rev. Lett. **113**, 246402 (2014).
[16] M. Neupane, S.-Y. Xu, R. Sankar, N. Alidoust, G. Bian, C. Liu, I. Belopolski, T.-R. Chang, H.-T. Jeng, H. Lin, A. Bansil, F. Chou, and M. Z. Hasan, Nat. Commun. **5**, 3786, (2014).
[17] Z. K. Liu, B. Zhou, Y. Zhang, Z. J. Wang, H. M. Weng, D. Prabhakaran, S.-K. Mo, Z. X. Shen, Z. Fang, X. Dai, Z. Hussain, and Y. L. Chen, Science **343**, 864 (2014).
[18] Z. K. Liu, J. Jiang, B. Zhou, Z. J. Wang, Y. Zhang, H. M. Weng, D. Prabhakaran, S. K. Mo, H. Peng, P. Dudin, T. Kim, M. Hoesch, Z. Fang, X. Dai, Z. X. Shen, D. L. Feng, Z. Hussain, and Y. L. Chen, Nat. Mater. **13**, 677 (2014).
[19] X. Wan, A. M. Turner, A. Vishwanath, and S. Y. Savrasov, Phys. Rev. B **83**, 205101 (2011).
[20] G. Xu, H. Weng, Z. Wang, X. Dai, and Z. Fang, Phys. Rev. Lett. **107**, 186806 (2011).
[21] A. A. Burkov and L. Balents, Phys. Rev. Lett. **107**, 127205 (2011).
[22] L. Balents, Physics **4**, 36 (2011).
[23] S. Murakami, New J. Phys. **9**, 356 (2007).
[24] G. B. Halász and L. Balents, Phys. Rev. B **85**, 035103 (2012).
[25] L. Lu, Z. Wang, D. Ye, L. Ran, L. Fu, J. D. Joannopoulos, and M. Soljacic, Science **349**, 622 (2015).
[26] J. Liu and D. Vanderbilt, Phys. Rev. B **90**, 155316 (2014).
[27] M. Hirayama, R. Okugawa, S. Ishibashi, S. Murakami, and T. Miyake, Phys. Rev. Lett. **114**, 206401 (2015).
[28] H. Weng, C. Fang, Z. Fang, B. A. Bernevig, and X. Dai, Phys. Rev. X **5**, 011029 (2015).
[29] S.-M. Huang, S.-Y. Xu, I. Belopolski, C.-C. Lee, G. Chang, B. Wang, N. Alidoust, G. Bian, M. Neupane, C. Zhang, S. Jia, A. Bansil, H. Lin, and M. Z. Hasan, Nat. Commun. **6**, 7373 (2015).
[30] B. Q. Lv, N. Xu, H. M. Weng, J. Z. Ma, P. Richard, X. C. Huang, L. X. Zhao, G. F. Chen, C. E. Matt, F. Bisti, V. N. Strocov, J. Mesot, Z. Fang, X. Dai, T. Qian, M. Shi, and H. Ding, Nat. Phys. **11**, 724 (2015).
[31] B. Q. Lv, H. M. Weng, B. B. Fu, X. P. Wang, H. Miao, J. Ma, P. Richard, X. C. Huang, L. X. Zhao, G. F. Chen, Z. Fang, X. Dai, T. Qian, and H. Ding, Phys. Rev. X **5**, 031013 (2015).
[32] L. X. Yang, Z. K. Liu, Y. Sun, H. Peng, H. F. Yang, T. Zhang, B. Zhou, Y. Zhang, Y. F. Guo, M. Rahn, D. Prabhakaran, Z. Hussain, S.-K. Mo, C. Felser, B. Yan, and Y. L. Chen, Nat. Phys. **11**, 728 (2015).
[33] X. Huang, L. Zhao, Y. Long, P. Wang, D. Chen, Z. Yang, H. Liang, M. Xue, H. Weng, Z. Fang, X. Dai, and G. Chen, Phys. Rev. X **5**, 031023 (2015).
[34] S.-Y. Xu, N. Alidoust, I. Belopolski, Z. Yuan, G. Bian, T.-R. Chang, H. Zheng, V. N. Strocov, D. S. Sanchez, G. Chang, C. Zhang, D. Mou, Y. Wu, L. Huang, C.-C. Lee, S.-M. Huang, B. Wang, A. Bansil, H.-T. Jeng, T. Neupert, A. Kaminski, H. Lin, S. Jia, and M. Zahid Hasan, Nat. Phys. **11**, 748 (2015).
[35] S.-Y. Xu, I. Belopolski, N. Alidoust, M. Neupane, G. Bian, C. Zhang, R. Sankar, G. Chang, Z. Yuan, C.-C. Lee, S.-M. Huang, H. Zheng, J. Ma, D. S. Sanchez, B. Wang, A. Bansil, F. Chou, P. P. Shibayev, H. Lin, S. Jia, and M. Z. Hasan, Science **349**, 613 (2015).
[36] B. Q. Lv, S. Muff, T. Qian, Z. D. Song, S. M. Nie, N. Xu, P. Richard, C. E. Matt, N. C. Plumb, L. X. Zhao, G. F. Chen, Z. Fang, X. Dai, J. H. Dil, J. Mesot, M. Shi, H. M. Weng, and H. Ding, Phys. Rev. Lett. **115**, 217601 (2015).
[37] N. Xu, H. M. Weng, B. Q. Lv, C. Matt, J. Park, F. Bisti, V. N. Strocov, D. gawryluk, E. Pomjakushina, K. Conder, N. C. Plumb, M. Radovic, G. Autès, O. V. Yazyev, Z. Fang, X. Dai, G. Aeppli, T. Qian, J. Mesot, H. Ding, and M. Shi, Nat. Commun. **7**, 11006 (2016).
[38] C. Zhang, Z. Yuan, S. Xu, Z. Lin, B. Tong, M. Z. Hasan, J. Wang, C. Zhang, and S. Jia, arXiv:1502.00251 (2015).
[39] Y. H. Wang, D. Hsieh, D. Pilon, L. Fu, D. R. Gardner, Y. S. Lee, and N. Gedik, Phys. Rev. Lett. **107**, 207602 (2011).
[40] Y. Wang and N. Gedik, Phys. Status Solidi RRL **7**, 64 (2013).
[41] M. Sentef, M. Claassen, A. Kemper, B. Moritz, T. Oka, J. Freericks, and T. Devereaux, Nat. Commun. **6**, 7047 (2015).
[42] E. J. Sie, J. W. McIver, Y.-H. Lee, L. Fu, J. Kong, and N. Gedik, Nat. Mater. **14**, 290 (2015).
[43] C. Ching-Kit, P. A. Lee, K. S. Burch, J. H. Han, and Y. Ran, Phys. Rev. Lett. **116**, 026805 (2016).
[44] C. Kunz, in *Photoemission in Solids II*, edited by L. Ley and M. Cardona (Springer-Verlag, Berlin, 1979).